Available online at www.sciencedirect.com
ScienceDirect
Chinese Journal of Natural Medicines 2023, **21**(12): 902-915
doi: 10.1016/S1875-5364(23)60441-8
Chinese Journal of Natural Medicines

•Original article•

Artemdubinoids A–N: novel sesquiterpenoids with antihepatoma cytotoxicity from *Artemisia dubia*

GAO Zhen[1, 2], LI Tianze[1], MA Yunbao[1], HUANG Xiaoyan[1], GENG Changan[1], ZHANG Xuemei[1], CHEN Jijun[1, 2*]

[1] *State Key Laboratory of Phytochemistry and Plant Resources in West China, Kunming Institute of Botany, Chinese Academy of Sciences, Kunming 650201, China;*
[2] *University of Chinese Academy of Sciences, Beijing 100049, China*

Available online 20 Dec., 2023

[ABSTRACT] In pursuit of effective agents for hepatocellular carcinoma derived from the *Artemisia* species, this study built upon initial findings that an ethanol (EtOH) extract and ethyl acetate (EtOAc) fraction of the aerial parts of *Artemisia dubia* Wall. ex Bess. exhibited cytotoxicity against HepG2 cells with inhibitory rates of 57.1% and 84.2% (100 μg·mL^{-1}), respectively. Guided by bioactivity, fourteen previously unidentified sesquiterpenes, artemdubinoids A–N (**1**–**14**), were isolated from the EtOAc fraction. Their structural elucidation was achieved through comprehensive spectroscopic analyses and corroborated by the comparison between the experimental and calculated ECD spectra. Single crystal X-ray diffraction provided definitive structure confirmation for artemdubinoids A, D, F, and H. Artemdubinoids A and B (**1**–**2**) represented unique sesquiterpenes featuring a 6/5-fused bicyclic carbon scaffold, and their putative biosynthetic pathways were discussed; artemdubinoid C (**3**) was a novel guaianolide derivative that might be formed by the [4 + 2] Diels–Alder reaction; artemdubinoids D and E (**4**–**5**) were rare 1,10-*seco*-guaianolides; artemdubinoids F–K (**6**–**11**) were chlorine-containing guaianolides. Eleven compounds exhibited cytotoxicity against three human hepatoma cell lines (HepG2, Huh7, and SK-Hep-1) with half-maximal inhibitory concentration (IC_{50}) values spanning 7.5−82.5 μmol·L^{-1}. Artemdubinoid M (**13**) exhibited the most active cytotoxicity with IC_{50} values of 14.5, 7.5 and 8.9 μmol·L^{-1} against the HepG2, Huh7, and SK-Hep-1 cell lines, respectively, which were equivalent to the positive control, sorafenib.

[KEY WORDS] Artemdubinoids A–N; *Artemisia dubia*; Sesquiterpenoids; Antihepatoma activity
[CLC Number] R284.1 **[Document code]** A **[Article ID]** 2095-6975(2023)12-0902-14

Introduction

The genus *Artemisia* (Asteraceae) is comprised of plants recognized for their medicinal properties and encompasses approximately 380 species, with 186 species flourishing in China [1]. Extensive phytochemical research has confirmed the genus as a prolific source of sesquiterpenoids, such as cadinene, germacrane, guaianolide, and bisabolane [2-6]. These compounds exhibited a broad range of biological effects, such as anticancer, antioxidant, antiviral, antifungal, antimicrobial, and antiinflammatory effects [7-12]. For instance, artemisinin, the lead molecule isolated from *A. annua*, serves as a celebrated antimalaria medication, and its derivatives, dihydroartemisinin and artesunate, also exhibit anticancer effects *via* the generation of reactive oxygen species, apoptosis induction, angiogenesis inhibition, and cell cycle arrest [13, 14]. Moreover, arglabin, a guaianolide from *A.glabella* and its derivative, dimethylamino hydrochloride, has been clinically approved in in Kazakhstan for the treatment of various cancers, including those of the breast, colon, ovary, and lung [15]. In our ongoing exploration for potential antihepatoma agents from Artemisia species, previous work uncovered four guaiane-guaiane dimer compounds (artemisinins A, J, K and lavandiolide H) with obvious cytotoxicity, displaying IC_{50} values of 4.4, 7.6, 6.7 and 3.8 μmol·L^{-1} against HepG2 cells, 9.6, 6.6, 6.0 and 4.6 μmol·L^{-1} against SMMC-7721 cells, and 7.6, 6.9, 5.6 and 4.5 μmol·L^{-1} against Huh7 cells. Detailed mechanism analysis revealed that lavandiolide H dose-de-

[Received on] 16-Mar.-2023
[Research funding] This work was supported by the Key Program of the National Natural Science Foundation of China (No. 22137008), the Xingdian Yingcai Project (No. YNWR-KJLJ-2019-002), the Youth Innovation Promotion Association, CAS (No. 2020386), the Reserve Talents of Young and Middle-aged Academic and Technical Leaders in Yunnan Province (No. 202105AC160021), and the State Key Laboratory of Phytochemistry and Plant Resources in West China (P2021-ZZ06).
[*]**Corresponding author]** E-mail: chenjj@mail.kib.ac.cn
These authors have no conflict of interest to declare.

pendently inhibited cell migration and invasion, induced G_2/M cell cycle arrest, and promoted HepG2 cell apoptosis. It also led to the downregulation of BCL-2 and PARP-1 expressions and activated PARP-1 to upregulate cleaved PARP-1 expression [16]. Artematrolide A demonstrated significant cytotoxic effects on cervical cancer cells by activating the ROS/ERK/mTOR signaling pathway and promoting metabolic shift [17]. Additionally, two novel cagelike sesquiterpenoids formed *via* intramolecular Diels−Alder cycloaddition and 16 unreported guaiane-type sesquiterpenoids from *A. atrovirens* exhibited cytotoxic effects on the HepG2, Huh7, and SMMC-7721 cell lines [18, 19]. Twenty novel sesquiterpenolides (including germacranolides, guaianolides, and eudesmanolides) identified in *A. myriantha* exhibited moderate cytotoxicity against three human hepatoma cell lines (HepG2, Huh7 and SMMC-7721), and artemyrianolide H displayed significant cytotoxicity against three tested cell lines with IC_{50} values of 4.9, 4.3 and 3.1 μmol·L^{-1}, respectively [1, 20].

Artemisia dubia (*A. dubia*) has long been traditionally employed in Chinese herbal medicine for treating acute fevers, coughs related to pulmonary heat, inflamed sore throats, epistaxis, rubella, and enterobiasis [21]. Previous phytochemical explorations of this species have identified over 70 compounds, predominantly sesquiterpenoids, within the guaiane, eudesmane, germane, and farnesene categories. Our preliminary investigations demonstrated that the ethanol (EtOH) fraction of *A. dubia* and its ethyl acetate (EtOAc) fraction showed cytotoxicity against HepG2 cells with inhibitory rates of 57.1% and 84.2% at a concentration of 100 μg·mL^{-1}. However, to date, detailed inquiries into the cytotoxic constituents of *A. dubia* are scant, with only a select number of guaianolides reported to exhibit mild cytotoxicity against Colo205 and MDA-MB-435 cell lines [21]. As part of ongoing efforts to discover bioactive compounds from *A. dubia*, this study successfully isolated fourteen unreported sesquiterpenoids, namely artemdubinoids A–N (**1**–**14**), from the active fractions. Compounds **1** and **2** feature a novel 6/5-fused bicyclic sesquiterpene scaffold, and compounds **3**–**14** are guaiane-type sesquiterpenoids with versatile structural diversity. Biological assays suggested that compound **13** showed the most potent cytotoxicity with IC_{50} values of 14.5, 7.5 and 8.9 μmol·L^{-1} against the HepG2, Huh7, and SK-Hep-1 cell lines, respectively. Herein, the isolation, structural elucidation, and cytotoxic activities of these newly identified compounds were described.

Results and Discussion

Artemdubinoid A (**1**) (Fig. 1), an orthorhombic crystal, possessed a molecular formula of $C_{17}H_{24}O_4$, deduced from the (+)-high-resolution electrospray ionization mass spectrometry (HR-ESI-MS) data at *m/z* 293.174 4 ([M + H]$^+$, Calcd. for 293.1747), corresponding to six degrees of unsaturation. Its infrared (IR) spectrum exhibited absorption bands at 3436, 1743, 1715, and 1625 cm^{-1}, indicating the existence of hydroxy, carbonyl, and olefinic groups. The ^{1}H nuclear magnetic resonance (NMR) data (Table 1) revealed characteristic signals for five olefinic protons δ_H 6.38 (1H, s), 5.98 (1H, s), 5.01 (1H, d, *J* = 10.9 Hz), 4.99 (1H, d, *J* = 2.7 Hz), and 5.80 (1H, dd, *J* = 17.6, 10.9 Hz), an oxygenated methylene proton δ_H 4.17 (2H, m), an oxygenated methine proton δ_H 4.08 (1H, d, *J* = 3.1 Hz), three methyl groups δ_H 1.28 (3H, t, *J* = 7.2 Hz), 1.13 (3H, d, *J* = 7.4 Hz), and 1.07 (3H, s). The corresponding ^{13}C NMR spectrum disclosed 17 carbon resonances, classified three methyls, five methylenes (two olefinic and one oxygenated), four methines (one olefinic and one oxygenated), and five quaternary carbons (one ketone carbonyl, and one ester carbonyl). The two double bonds and two carbonyls accounted for four indices of hydrogen deficiency, and the two remained degrees of unsaturation suggested that compound **1** had two other rings. The ^{1}H-^{1}H correlation spectroscopy (COSY) correlations of H-1' (δ_H 4.17)/H-2' (δ_H 1.28) and the heteronuclear multiple bond correlation (HMBC) between H-1' and C-12 (δ_C 167.8) indicated the existence of one ethoxy group (Fig. 2) . Apart from the substituents, 15 carbon resonances remained, which were indicative of a sesquiterpene backbone. The ^{1}H-^{1}H COSY correlations revealed three coupling systems, including H-1/H-2, H-8/H-9, and H-3/H-4/H-5. The key HMBCs of H-14 (δ_H 1.07) with C-10 (δ_C 49.0), C-1 (δ_C 143.6), C-5 (δ_C 65.2), and C-9 (δ_C 29.3), of H-8 (δ_H 1.70, 2.28) with C-10, C-6 (δ_C 213.7), and C-7 (δ_C 58.3), and of H-5 (δ_H 1.77) with C-10, C-1, C-6, and C-7 led to the establishment of a six-membered ring (ring A) (Fig. 3). Similarly, the HMBC correlations from H-15 (δ_H 1.13) to C-3 (δ_C 79.2), C-4 (δ_C 38.1), C-5 (δ_C 65.2) and from H-3 (δ_H 4.08) to C-4, C-5, C-6, and C-7 constructed a five-membered ring (ring B). Additionally, the positions of the remaining carbons were assigned by the correlations of H-13 (δ_H 6.38, 5.98) with C-7, C-11 (δ_C 139.7), and C-12. Thus, the planar structure of **1** was constructed as a 6/5-fused bicyclic sesquiterpene featuring an unprecedented carbon scaffold.

Due to the insufficient signals in the rotating frame Overhauser effect spectroscopy (ROESY) spectra except for the correlations between H-14 and H-5, the relative configuration of compound **1** could not be resolved conclusively. Single crystals of **1** were obtained in CH_3OH–$CHCl_3$ (5 ∶ 95) and performed on an X-ray diffraction experiment using Cu Kα radiation to confirm its absolute configuration as 1*S*,4*S*,5*R*,6*S*,8*R*. Therefore, the structure of **1** was unequivocally determined and named artemidubianolide A.

Artemdubinoid B (**2**), a white powder, was established to have a molecular formula of $C_{16}H_{22}O_4$ as determined by the (+)-HR-ESI-MS *m/z* 279.1596 [M + H]$^+$ (Calcd. for $C_{16}H_{23}O_4$, 279.1591). The NMR data of compound **2** resembled those of compound **1**, except that the ethoxy at C-12 in **1** was replaced by a methoxy in **2**. This deduction was supported by the characteristic NMR signals, as well as the HMBCs between H-OMe (δ_H 3.55) and C-12 (δ_C 129.1). The analyses of the ROESY signals and electronic circular dichroism (ECD) spectra showed that the absolute configuration of **2** was identical to those of **1**. Hence, the structure of com-

Table 1 ^{1}H NMR data for compounds 1–7 (δ in ppm, *J* in Hz)

No.	1[a]	2[a]	3[a]	4[c]	5[c]	6[c]	7[d]
1	5.80 (dd, 17.6, 10.9)	5.82 (dd, 17.5, 11.0)					
2	5.01 (d, 10.9)	5.04 (d, 6.0)	5.83 (overlapped)	2.68 (m)	2.77 (dd, 18.3, 6.3)	2.49 (dd, 13.3, 13.3)	2.18 (m)
	4.99 (d, 2.7)	5.01 (s)		2.42 (m)	2.22 (dd, 18.3, 2.4)	2.01 (m)	2.11 (m)
3	4.08 (d, 3.1)	4.09 (s)	5.83 (overlapped)		4.67 (m)	4.45 (dd, 12.8, 6.7)	4.22 (overlapped)
4	2.25 (qd, 7.4, 3.1)	2.25 (m)					
5	1.77 (s)	1.80 (s)	3.23 (m)			2.26 (d, 11.5)	2.41 (d, 10.9)
6			4.11 (dd, 10.0, 10.0)	5.08 (d, 7.3)	5.06 (d, 6.8)	4.09 (dd, 11.5, 8.7)	4.22 (overlapped)
7			2.24 (m)	3.23 (m)	2.66 (m)	2.97 (m)	3.37 (m)
8	2.28 (m)	2.30 (m)	1.47 (m)	1.75 (m)	1.76 (m)	2.84 (m)	2.72 (m)
	1.70 (m)	1.72 (m)	2.29 (m)	1.51 (m)	1.48 (m)	2.34 (m)	2.05 (m)
9	2.08 (m)	2.11 (m)	1.85 (m)	2.74 (m)	2.55 (m)	2.29 (m)	5.46 (m)
	1.62 (m)	1.65 (m)		2.56 (m)		1.38 (m)	
11				2.95 (m)	2.92 (m)		
13	6.38 (s)	6.41 (s)	6.09 (d, 3.5)	1.22 (d, 7.6)	1.20 (d, 7.6)	6.15 (d, 3.5)	6.07 (d, 3.5)
	5.98 (s)	6.04 (s)	5.36 (d, 3.5)			5.62 (d, 3.5)	5.53 (d, 3.5)
14	1.07 (s)	1.09 (s)	1.34 (s)	2.14 (s)	2.13 (s)	5.13 (s)	1.76 (s)
						5.11 (s)	
15	1.13 (d, 7.4)	1.15 (d, 7.4)	1.51 (s)	2.23 (s)	2.20 (s)	1.28 (s)	1.13 (s)
1'	4.17 (m)	3.55 (s)	2.30 (dd, 11.2, 9.6)				
			1.37 (dd, 11.2, 5.3)				
2'	1.28 (t, 7.2)		2.98 (dd, 9.6, 5.3)				
4'			2.39 (m)				
			2.37 (m)				
5'			1.54 (m)				
			1.47 (m)				
6'			1.26 (m)				
			1.24 (m)				
7'			1.30 (m)				
			1.28 (m)				
8'			0.89 (t, 7.3)				

[a]Recorded in $CDCl_3$; [b]Recorded in pyridine-d_5; [c]Recorded in CD_3OD; [d]Recorded in $(CD_3)_2CO$

pound **2** was elucidated.

Structurally, artemdubinoids A and B (**1**–**2**) represented unique sesquiterpenes featuring a 6/5-fused bicyclic carbon scaffold, and their plausible biosynthetic pathways were proposed as shown in Scheme 1. Compounds **1** and **2** might be derived from the same precursor germacranolide **i**, which underwent Cope rearrangement to form **ii**, followed by oxidation, hydrolysis, and re-oxidation to form **iii**, and the **iii** was further transformed into intermediate **iv** by an aldol reaction. Finally, **iv** was methylated and ethylated to yield compounds **1** and **2** (Scheme 1).

Artemdubinoid C (**3**) was isolated as a colorless oil and assigned a molecular formula of $C_{23}H_{32}O_4$, deduced from the (–)-HR-ESI-MS data at *m/z* 417.2287 ([M + HCOO]$^-$, Calcd. for 417.2283), implying eight indices of hydrogen deficiency. The IR spectrum indicated the presence of hydroxy (3439 cm^{-1}) and carbonyl groups (1758 and 1706 cm^{-1}). The ^{1}H NMR spectrum (Table 1) showed signals ascribed to three methyls at δ_H 1.34 (3H, s), 1.51 (3H, s), and 0.89 (3H, t, *J* = 7.3 Hz), a pair of exocyclic methylene protons at δ_H 6.09 (1H, d, *J* = 3. 5Hz) and 5.36 (1H, d, *J* = 3.5 Hz), two olefinic protons at δ_H 5.83 (1H, overlapped) and 5.83 (1H, overlapped), one oxygenated methine at δ_H 4.11 (1H, dd, *J* = 10.0, 10.0 Hz). The ^{13}C NMR spectrum (Table 3) displayed 23 resonances classified as three methyls, eight methylenes (one olefinic carbon), six methines (two olefinic carbons and one

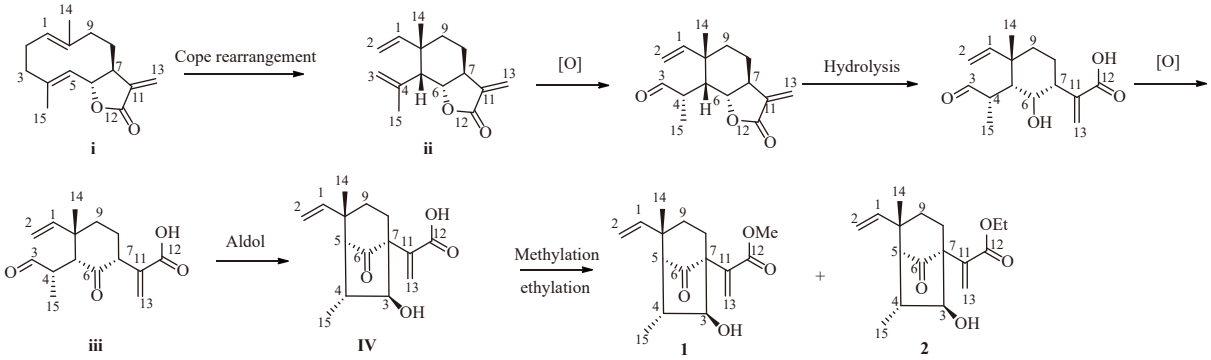

Scheme 1 Plausible biosynthetic pathways of compounds 1 and 2.

oxygenated), and six quaternary carbons (one oxygenated carbon, one olefinic carbon, and two carbonyl carbons). The ^{1}H-^{1}H COSY correlations of H-8'/H-7'/H-6'/H-5'/H-4' and H-1'/H-2', together with the HMBCs between H-4' (δ_H 2.39, 2.37) and C-3' (δ_C 211.5) and between H-2' (δ_H 2.98) and C-3', suggested the presence of an undecan-3-one. In addition to the assigned signals for the undecan-3-one moiety, the remained 15 carbon resonances were pointed to a sesquiterpenoid scaffold. The ^{1}H-^{1}H COSY spectrum displayed two coupling systems, which were H-2/H-3 and H-5/H-6/H-7/H-8/H-9. In the HMBC spectrum, the correlations of H-13 with C-7 and C-12 and of H-7 with C-12 and C-13 indicated the existence of an *α*-methylene-*γ*-lactone moiety. The key HMBCs of H-5 with C-2, C-3, C-7, and C-10, of H-6 with C-1 and C-8, of H-9 with C-1 and C-7, of H-14 with C-1, C-9, and C-10, and of H-15 with C-3, C-4, and C-5 established **3** as a charac-

Table 2 ^{1}H NMR data for compounds 8–14 (δ in ppm, *J* in Hz)

No.	8[a]	9[a]	10[b]	11[d]	12[a]	13[a]	14[a]
1		3.39, m					2.54, m
2	3.00, d, (16.8)	2.77, m	3.28, m	6.09, dd, (2.8, 2.8)	6.26, d, (1.8)	6.23, t, (2.8)	1.95, m
	2.37, d, (16.8)	2.07, m	2.16, m	4.43, dd, (6.9, 2.8)			1.69, m
3	4.13, d, (4.2)	4.53, overlapped	4.57, d, (4.3)		6.23, d, (1.8)	2.92, m	5.43, d, (1.8)
4							
5	2.93, d, (9.5)	2.96, t, (11.4)	3.08, d, (10.6)	3.29, dd, (10.5, 2.8)	5.21, d, (10.6)		2.74, d, (9.6)
6	4.31, t, (10.1)	4.54, overlapped	4.54, dd, (10.6, 8.8)	4.57, dd, (10.1, 10.1)	3.69, dd, (10.6, 9.4)	5.21, d, (9.9)	4.11, dd, (10.0, 10.0)
7	2.32, m	2.82, m	3.33, dd, (14.5, 4.3)	2.98, m	3.63, m	2.59, m	3.18, m
8	1.74, m	2.10, m	3.15, td, (12.9, 4.5)	2.14, m	2.34, m	1.97, m	2.23, m
	1.39, m	1.24, m	2.25, td, (12.9, 3.8)	1.83, m	1.50, m		1.44, m
9	2.20, m	2.55, m	2.13, m	1.95, m	2.14, m	2.12, m	1.94, m
		1.85, m	1.31, m	1.81, m	1.61, m	1.63, m	1.69, m
10							
11	2.66, m						
12							
13	1.18, d, (7.8)	6.30, d, (3.3)	6.31, d, (3.5)	6.04, d, (3.5)	6.18, d, (3.6)	6.09, d, (2.0)	6.13, d, (3.3)
		5.48, d, (3.3)	5.49, d, (3.5)	5.55, d, (3.2)	5.44, d, (3.6)	5.50, d, (3.5)	5.30, d, (3.3)
14	1.74, s	5.19, s	5.31, s	1.49, s	1.48, s	1.46, s	1.17, s
		5.07, s	5.15, s				
15	1.86, s	2.13, s	2.18, s	1.86, s	2.19, s	2.19, s	1.84, s
-OMe					3.14, s		

[a]Recorded in $CDCl_3$; [b]Recorded in pyridine-d_5; [d]Recorded in $(CD_3)_2CO$

Table 3 ^{13}C NMR data for compounds **1**–**14** (δ in ppm)

No.	1[a]	2[a]	3[a]	4[c]	5[c]	6[c]	7[d]	8[a]	9[a]	10[b]	11[d]	12[a]	13[a]	14[a]
1	143.6, CH	143.4, CH	64.7, C	210.3, C	205.8, C	78.7, C	76.7, C	133.2, C	44.9, CH	83.4, C	153.1, C	148.2, C	134.9, C	54.3, CH
2	112.4, CH_2	112.2, CH_2	134.1, CH	35.7, CH_2	45.5, CH_2	45.9, CH_2	48.2, CH_2	39.7, CH_2	37.1, CH_2	45.8, CH_2	128.2, CH	131.9, CH	128.1, CH	34.0, CH_2
3	79.2, CH	79.0, CH	136.5, CH	33.5, CH_2	72.0, CH	66.5, CH	66.0, CH	80.1, CH	82.8, CH	84.4, CH	84.2, CH	127.7, CH	45.9, CH_2	126.0, CH
4	38.1, CH	38.0, CH	57.0, C	179.2, C	176.3, C	81.6, C	81.0, C	81.4, C	83.2, C	84.4, C	81.2, C	148.6, C	148.0, C	142.6, C
5	65.2, CH	65.0, CH	70.6, CH	136.5, C	137.5, C	64.8, CH	67.6, CH	55.5, CH	53.9, CH	65.2, CH	60.1, CH	60.2, C	137.1, C	54.7, CH
6	213.7, C	213.4, C	80.0, CH	78.8, CH	78.5, CH	84.5, CH	80.4, CH	83.0, CH	84.5, CH	82.8, CH	81.7, CH	83.0, CH	83.0, CH	84.8, CH
7	58.3, C	58.1, C	43.4, CH	43.4, CH	43.7, CH	48.0, CH	41.2, CH	49.3, CH	47.7, CH	46.5, CH	47.8, CH	43.8, CH	48.7, CH	44.0, CH
8	32.3, CH_2	32.2, CH_2	23.9, CH_2	22.2, CH_2	22.2, CH_2	32.2, CH_2	33.1, CH_2	24.4, CH_2	32.6, CH_2	31.4, CH_2	23.1, CH_2	24.1, CH_2	40.2, CH_2	35.2, CH_2
9	29.3, CH_2	29.1, CH_2	35.2, CH_2	41.6, CH_2	41.6, CH_2	33.1, CH_2	126.0, CH	35.4, CH_2	40.2, CH_2	33.0, CH_2	38.5, CH_2	36.6, CH_2	75.2, CH_2	25.1, CH_2
10	49.0, C	49.0, C	73.3, C	210.6, C	210.6, C	152.3, C	137.6, C	131.4, C	148.4, C	152.2, C	71.1, C	77.2, C	75.2, C	74.3, C
11	139.7, C	139.2, C	141.2, C	39.2, CH	39.0, CH	140.8, C	141.2, C	39.8, CH	140.7, C	140.7, C	141.8, C	141.0, C	139.7, C	141.0, C
12	167.8, C	168.0, C	170.9, C	182.4, C	182.2, C	172.0, C	170.1, C	180.0, C	170.6, C	170.6, C	170.1, C	170.7, C	170.7, C	170.8, C
13	128.7, CH_2	129.0, CH_2	118.8, CH_2	10.9, CH_3	10.8, CH_3	121.1, CH_2	120.2, CH_2	10.4, CH_3	120.3, CH_2	120.3, CH_2	118.6, CH_2	119.4, CH_2	119.8, CH_2	119.8, CH_2
14	26.2, CH_3	26.0, CH_3	30.2, CH_3	30.0, CH_3	30.0, CH_3	115.0, CH_2	24.7, CH_3	24.9, CH_3	113.9, CH_2	115.0, CH_2	25.7, CH_3	25.5, CH_3	24.6, CH_3	30.2, CH_3
15	21.9, CH_3	21.7, CH_3	18.1, CH_3	17.8, CH_3	14.1, CH_3	17.2, CH_3	17.9, CH_3	25.5, CH_3	27.1, CH_3	27.6, CH_3	29.7, CH_3	17.5, CH_3	15.0, CH_3	17.5, CH_3
1'	61.3, CH_2	52.1, CH_2	34.0, CH_2									50.5, CH_3	50.0, CH_3	
2'	14.3, CH_3	-	58.4, CH											
3'			211.5, C											
4'			44.4, CH_2											
5'			23.6, CH_2											
6'			31.6, CH_2											
7'			22.7, CH_2											
8'			14.1, CH_3											

[a]Recorded in $CDCl_3$; [b]Recorded in pyridine-d_5; [c]Recorded in CD_3OD; [d]Recorded in $(CD_3)_2CO$

teristic guaianolide sesquiterpene. Since two carbonyls, one double bond, and a guaianolide scaffold accounted for six double-bond equivalents, the molecule required an additional ring to satisfy the remained one degree of unsaturation, suggesting that another ring was formed between the undecan-3-one moiety and guaianolide sesquiterpene scaffold. These inferences were further supported by the observed HMBCs of H-1' with C-1 and C-2 and of H-2' with C-3 and C-4. Therefore, the planar structure of **3** was concluded.

The relative configuration of **3** was inferred based on its ROESY spectrum and coupling constants. In natural guaiane-type sesquiterpenoids, H-7 typically maintains an *α*-orientation [21], and the large coupling constants of H-5/H-6 (J = 10.0 Hz) and H-6/H-7 (J = 10.0 Hz) suggests their *trans* relationships. In the ROESY spectrum, the correlations of H-7/H-5, H-5/H-2', and H-7/H-15 demonstrated an *α*-orientation for H-5, H-15 and H-2', while the correlations of H-2/H-6, H-2/H-14, H-6/H-14 and H-14/H-1'a proposed a *β*-orientation for H-14 and H-1'. Its absolute configuration was confirmed to be 1*R*,4*R*,5*S*,6*S*,7*S*,10*R*,2'*S* by the good agreement between the experimental and calculated ECD spectra.

Artemdubinoid D (**4**) was isolated as a colorless crystal with a molecular formula of $C_{15}H_{20}O_4$ based on the analysis of the (+)-HR-ESI-MS data at *m/z* 287.123 0 ($[M + Na]^+$, Calcd. for 287.125 4), accounting for six degrees of unsaturation. Its IR spectrum exhibited absorption bands for carbonyl (1771 cm^{-1}) and olefinic groups (1648 cm^{-1}). Detailed analyses of the 1D and 2D NMR data of **4** (Table 1) fully constructed the planar structure, which was identical to that of 3-deshydroxy-*iso*-*seco*-tanapartholide [22]. However, the coupling constant ($J_{H\text{-}6/H\text{-}7}$ = 7.3 Hz) of **4** was different from that of 3-deshydroxy-*iso*-*seco*-tanapartholide ($J_{H\text{-}6/H\text{-}7}$ = 9.5 Hz), which suggested a configurational difference between the two compounds. The relative conformations of H-7 and H-6 are usually deduced according to a well-established principle and *J*-based analyses. This principle suggests that in natural guaianolides, H-7 always has the *α*-orientation, while the large coupling constant ($J_{H\text{-}6/H\text{-}7} \geq$ 9.5 Hz) indicates that H-6 and H-7 are in the *trans*-configuration, but the relative configuration of **4** could not be determined from the theory mentioned above due to the medium coupling constant ($J_{H\text{-}6/H\text{-}7}$ = 7.3 Hz). Single crystals of **4** were obtained in CH_3OH–$CHCl_3$ (5 ∶ 95) and subjected to an X-ray diffraction experiment with Cu K*α* radiation, which confirmed the structure and absolute configuration of **4** and named as artemidubinoid D. In addition, we corrected the published structure of 1,10-secoguaianolide **1**. Analyses of the single crystal data show that if the coupling constant between H-6 and H-7 is around 7.3 Hz, they are in fact still in the *trans*-configuration.

Artemdubinoid E (**5**) had a molecular formula of $C_{15}H_{20}O_5$, deduced from (–)-HR-ESI-MS *m/z* 325.1284 $[M + HCOO]^-$ (Calcd. for $C_{16}H_{21}O_7$, 325.1293), indicating 16 Da more than compound **4**. The IR absorption bands at 3433, 1770 , and 1651 cm^{-1} indicated the presence of carbonyl and olefinic functionalities. The ^1H and ^{13}C NMR (Tables 1 and 3) spectral data of **5** were very similar to those of **4**, and the main difference was the presence of a hydroxy group in **5**. The location of the hydroxy group at C-3 was supported by the HMBCs of H-3 (δ_H 4.67) with C-2 (δ_C 45.5) and C-4 (δ_C 176.3). In the ROESY spectrum, the correlation between H-6/H-13 and H-3/H-11 indicated that H-13 was *β*-oriented while H-3 was in *α*-orientation. The absolute configuration was determined by the similarity between the experimental and calculated ECD spectra. Therefore, the absolute configuration of **5** was affirmed to be 3*S*,6*S*,7*S*,11*R*.

Artemdubinoid F (**6**), an orthorhombic crystal, was deduced to contain one chlorine atom based on the relative abundance ratios of 3 ∶ 1 for *m/z* 321.0852 ($[M + Na]^+$) and *m/z* 323.0815 ($[M + Na + 2]^+$) in the (+)-HR-ESI-MS. From the HR-ESI-MS spectra, compound **6** was identified to have a molecular formula of $C_{15}H_{19}O_4Cl$, corresponding to six degrees of hydrogen deficiency. The IR spectrum showed characteristic bands for hydroxy group (3346 cm^{-1}) and carbonyl (1763 cm^{-1}) functionalities. The ^1H NMR data (Table 1) showed the presence of two exomethylene groups at δ_H 6.15 (1H, d, J = 3.5 Hz), 5.62 (1H, d, J = 3.5 Hz), 5.13 (1H, s), and 5.11 (1H, s), one chlorinated methine at δ_H 4.45 (1H, dd, J = 12.8, 6.7 Hz), one oxygenated methine at δ_H 4.09 (1H, dd, J = 11.5, 8.7 Hz). The ^{13}C NMR spectrum (Table 3) presented 15 resonances, including one methyl, five methylenes, four methines, and five quaternary carbons. The aforementioned NMR data indicated a close resemblance to those of 1*α*,4*α*-dihydroxy-3*β*-chloro-8*α*-acetoxyguai-10(14), 11(13)-dien-6*α*,12-olide [23], except for the lack of an acetyl group at C-8. The above deduction was confirmed by the difference of 58 Da ($C_2H_2O_2$) between their molecular weights and 2D NMR data, including the ^1H-^1H COSY correlations of H-5 (δ_H 2.26)/H-6 (δ_H 4.09) /H-7 (δ_H 2.97) /H_2-8 (δ_H 2.84, 2.34), and H_2-9 (δ_H 2.29, 1.38) and HMBCs of H-8 with C-6 (δ_C 84.5), C-7 (δ_C 48.0), and C-9 (δ_C 33.1). Thus, the 2D structure of **6** was determined. By repeated crystallization from CH_3OH–$CHCl_3$ (5 ∶ 95) at room temperature, compound **6** was obtained as a suitable crystal for X-ray crystallographic diffraction experiment with Cu K*α* radiation to conclude compound **6** as (1*S*,3*S*,4*S*,5*R*,6*S*,7*S*)-1,4-dihydroxy-3-chloroguaian-10(14),11(13)-dien-12,6-olide.

Artemdubinoid G (**7**) was assigned the same molecular formula of $C_{15}H_{19}O_4Cl$ as compound **6** by the ratios of 3 ∶ 1 for *m/z* 321.0853 ($[M + Na]^+$) and *m/z* 323.0866 ($[M + Na + 2]^+$) in the (+)-HR-ESI-MS. The IR spectrum showed absorption bands for hydroxy (3426 cm^{-1}) and carbonyl (1758 cm^{-1}) functionalities. The ^1H and ^{13}C NMR data of **7** were similar to those of **6**, except for the absence of a terminal double-bond and the existence of an additional methine (δ_H 5.46/δ_C 126.9) and methyl (δ_H 1.76/δ_C 24.9). This analysis indicated that the exocyclic the $\Delta^{10(14)}$ double bond in **6** shifted to the Δ^9 double bond in **7**, which was verified by HMBCs of H_3-14 (δ_H 1.76) with C-1 (δ_C 77.1), C-9 (δ_C 126.9), and C-10 (δ_C 137.6). The relative configuration of **7** was deduced by the ROESY spectra and the correlations of H-3/H-5, H-5/H-7, and H-6/H-15

indicated H-15 and H-6 were *β*-oriented and H-3 was *α*-oriented. Combined with ECD calculations, compound **7** was established as (1*S*,3*S*,4*S*,5*R*,6*S*,7*S*)-1,4-dihydroxy-3-chloroguaian-9(10),11(13)-dien-12,6-olide.

Artemdubinoid H (**8**), an orthorhombic crystal with relative abundance ratios of 3 ∶ 1 for *m/z* 285.1272 ($[M + H]^+$) and *m/z* 287.1248 ($[M + H + 2]^+$) was observed in the (+)-HR-ESI-MS, suggesting that compound **8** also had a monochlorinated structure with the molecular formula of $C_{15}H_{21}O_3Cl$. The ^1H NMR spectrum showed the presence of three methyl group signals, including one doublet at δ_H 1.18 (3H, d, *J* = 7.8 Hz) and two singlets at 1.86 (3H, s) and 1.74 (3H, s) and two oxygenated methines at δ_H 4.31 (1H, dd, *J* = 10.1, 10.1 Hz) and 4.13 (1H, d, *J* = 4.2 Hz). The ^1H-^1H COSY spectrum pointed to two coupling systems in **8**, which were H-2/H-3 and H-5/H-6/H-7(H-11/H-13)/H-8/H-9. HMBCs of H-13 with C-7 (δ_C 49.3), C-11 (δ_C 39.8), and C-12 (δ_C 180.0), of H-14 with C-1 (δ_C 133.2), C-9 (δ_C 35.4), and C-10 (δ_C 131.4), and of H-15 with C-3 (δ_C 80.1), C-4 (δ_C 81.4), and C-5 (δ_C 55.5) indicated compound **8** was also a guaiane-type sesquiterpenoid. Due to the inadequate signals (except for the correlations between H-5/H-7 and H-6/H-13) in the ROESY spectrum, it was difficult to determine the relative configuration of **8**. Thus, the single crystals of **8** were obtained in CH_3OH–$CHCl_3$ (5 ∶ 95) and submitted to an X-ray diffraction experiment using Cu K*α* radiation, which defined its absolute configurations as 3*R*,4*R*,5*S*,6*S*,7*S*,11*R*.

Artemdubinoid I (**9**) was deduced to have a molecular formula of $C_{15}H_{19}O_3Cl$ by the relative abundance ratios of 3 ∶ 1 for *m/z* 283.1121 ($[M + H]^+$) and *m/z* 285.1101 ($[M + H + 2]^+$) in the (+)-HR-ESI-MS. The NMR data of compound **9** resembled those of **8**, indicating that they had a similar structure. By comparison of **9** with **8**, the main differences were the presence of two terminal double-bonds, an additional methine and the absence of a methyl in **9**. This analysis suggested that the $\Delta^{1(10)}$ double bond in **8** was shifted to the exocyclic $\Delta^{10(14)}$ double bond in **9** and the methyl at C-11 in **8** was changed to an exocyclic double bond in **9**, which was consistent with the HMBCs. The coupling constant of H-1/H-5 (*J* = 11.4 Hz) indicated their *trans* relationships. In the ROESY spectrum, the correlation of H-5/H-7 suggested H-1 was *β*-oriented. Moreover, the ECD calculations confirmed its absolute configuration. As shown in Fig. 4, the 1*S*,3*R*,4*R*,5*S*,6*S*,7*S* absolute configuration for **9** was determined from the similarities between the experimental and calculated ECD curves.

Artemdubinoid J (**10**) was assigned the molecular formula $C_{15}H_{19}O_4Cl$ by the ^{13}C NMR data and the relative abundance ratios of 3 ∶ 1 for *m/z* 299.1057 ($[M + H]^+$) and *m/z* 301.1053 ($[M + H + 2]^+$) in the (+)-HR-ESI-MS, requiring six indices of hydrogen deficiency. The ^1H and ^{13}C NMR data (Tables 2 and 3) of **10** closely resembled those of **9**, and the only difference was the presence of an additional hydroxy group in **10**. The C-1 location of the hydroxy group was confirmed by HMBCs of H_2-14 with C-1, C-9, and C-10. A convenient rule for rapidly determining the configuration of guaiane-type sesquiterpenes at C-1 is that the ECD spectra (MeOH) of sesquiterpenes (C1-*S*; 1-OH-*α*) exhibited obvious positive Cotton effects at 240 nm and relatively weak negative Cotton effects at 320 nm [24]. According to this rule combined with the ECD experimental curve of compound **10**, we assigned 1-OH as the *α*-configuration. The ROESY correlations of H-3/H-6, H-5/H-7, and H-7/H-15 indicated the relative configuration of **10**. The experimental and calculated ECD spectra were in good agreement (Fig. 4). Thus, the absolute configuration of **10** was determined to be 1*S*,3*R*,4*R*,5*R*,6*S*,7*S*.

Artemdubinoid K (**11**) was obtained as a white powder. Its molecular formula $C_{15}H_{19}O_4Cl$ was established by the relative abundance ratios of 3 ∶ 1 for *m/z* 299.1060 ($[M + H]^+$) and *m/z* 301.1097 ($[M + H + 2]^+$) in the (+)-HR-ESI-MS, indicating six degrees of unsaturation. The IR spectrum showed absorptions at 3424 and 1759 cm^{-1} due to hydroxy and carbonyl groups, respectively. The ^1H NMR spectrum displayed (Table 2) signals for three olefinics at δ_H 6.09 (1H, dd, *J* = 2.8, 2.8 Hz), 6.04 (1H, d, *J* = 3.5 Hz), and 5.55 (1H, d, *J* = 3.2 Hz), two oxymethine protons at δ_H 4.57 (1H, dd, *J* = 10.1, 10.1 Hz) and 4.43 (1H, dd, *J* = 6.9, 2.8 Hz), and two methyl protons at δ_H 1.86 (3H, s) and 1.49 (3H, s). The ^{13}C NMR data (Table 3) exhibited 15 carbon signals corresponding to one ester carbonyl, four quaternary carbons, three methylenes, five methines, and two methyls. These data suggested a guaiane-type sesquiterpenoid scaffold. The ^1H-^1H COSY spectrum revealed two spin systems, H-2/H-3 and H-5/H-6/H-7. The HMBCs of H-13 with C-7, C-11, and C-12, of H-14 with C-1, C-9, and C-10, and of H-15 with C-3, C-4, and C-5 (Fig. 2), in conjunction with the aforementioned COSY spin systems, confirmed the planar structure of **11**. The relative configuration of **11** was resolved by its coupling constants and ROESY correlations. In the ROESY spectrum, the correlations of H-7/H-14, OH-3/H-5, H-5/H-15, and H-5/H-7 indicated that these protons were on the same face with an *α*-orientation (Fig 3). The absolute configuration was determined from the similarity between the experimental and calculated ECD spectra. Thus, the structure of compound **11** was defined as 3*R*,4*R*,5*S*,6*S*,7*S*,10*S*.

Artemdubinoid L (**12**) was established to have a molecular formula of $C_{16}H_{20}O_3$ with seven double bond equivalents based on the (+)-HR-ESI-MS *m/z* 261.1110 $[M + H]^+$ (Calcd. for $C_{16}H_{21}O_3$, 261.1121). The IR spectrum indicated the existence of carbonyl (1765 cm^{-1}) and olefinic groups (1648 cm^{-1}). The ^1H NMR spectrum (Table 2) exhibited typical signals for two singlet methyl protons at δ_H 2.19 (3H, s) and δ_H 1.48 (3H, s), one methoxy proton at δ_H 3.14 (3H, s), two olefinic methylene protons at δ_H 6.18 (1H, d, *J* = 3.6 Hz) and δ_H 5.44 (1H, d, *J* = 3.6 Hz), one oxygenated methine proton at δ_H 3.69 (1H, dd, *J* = 10.6, 9.4 Hz), and two olefinic protons at δ_H 6.26 (1H, d, *J* = 1.8 Hz) and 6.23 (1H, d, *J* = 1.8 Hz). The ^{13}C NMR (DEPT) spectrum (Table 3) revealed 16 carbon resonances, including two methyls, one methoxy,

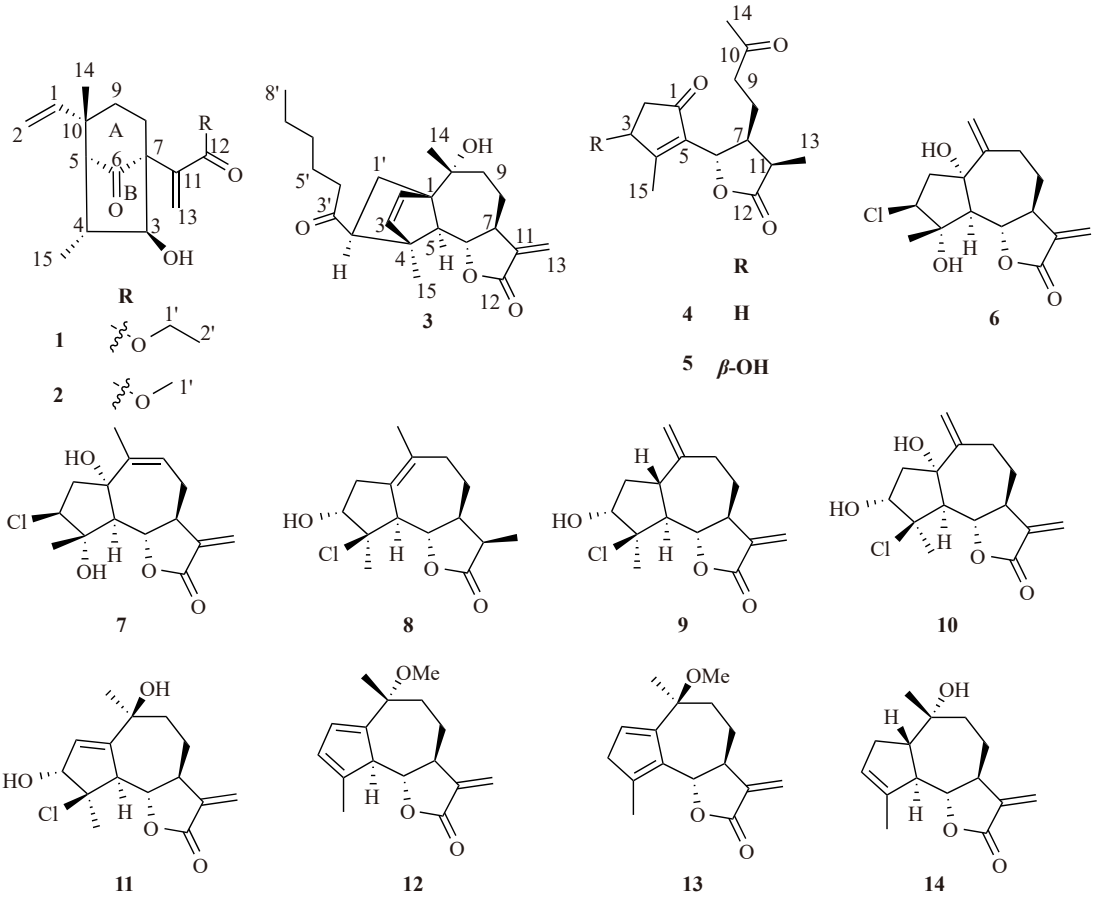

Fig. 1 Chemical structures of compounds 1–14.

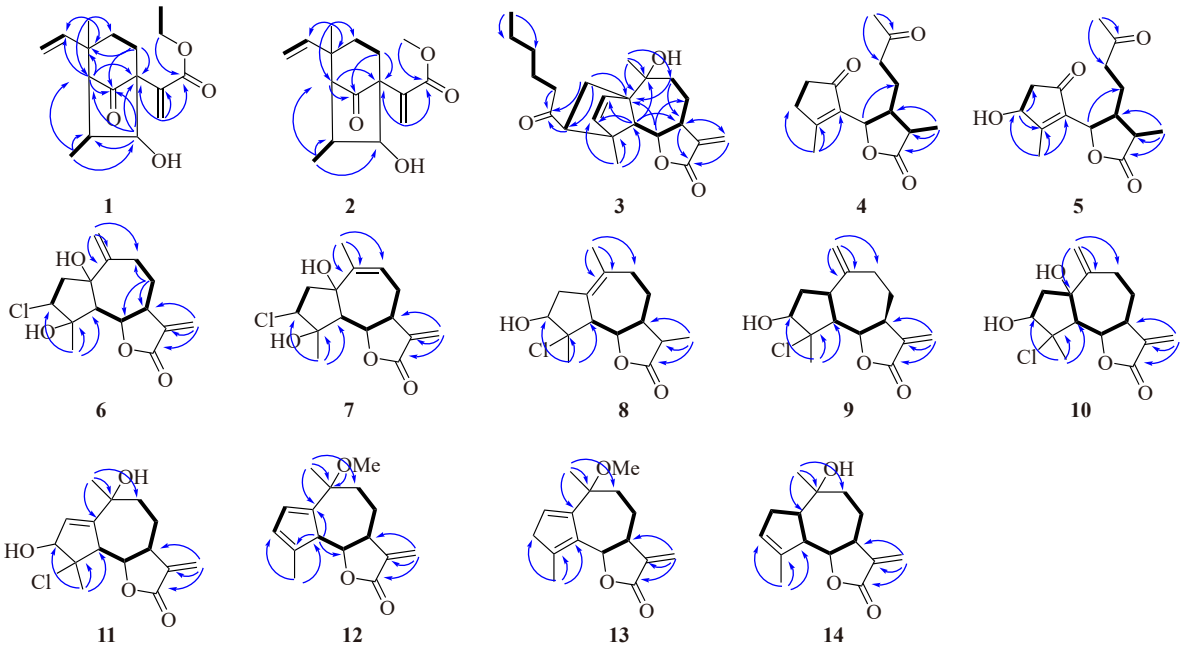

Fig. 2 Key ^{1}H–^{1}H COSY and HMBC correlations of compounds 1–14.

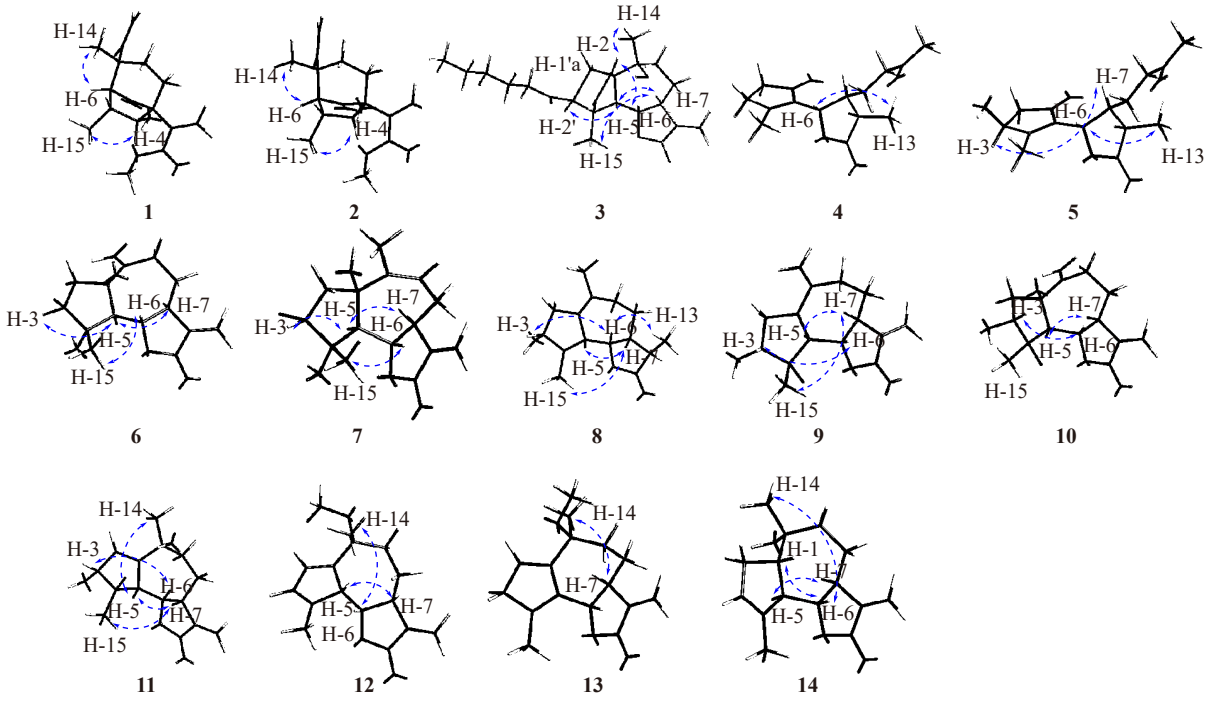

Fig. 3 Key ROESY correlations of compounds 1−14.

three methylenes, five methines (one oxygenated, two olefinic), five quaternary carbons (one oxygenated, three olefinic, and one ester carbonyl). Detailed analyses of the above characteristic signals revealed that **12** was a guaiane-type sesquiterpenoid containing a methoxy group.

The ^{1}H-^{1}H COSY spectrum revealed two coupling systems, including H-2/H-3 and H-5/H-6/H-7/H-8/H-9. The two coupling systems were connected by the key HMBCs cof H-5 (δ_H 5.21) with C-1 (δ_C 148.2), C-4 (δ_C 148.6), and C-6 (δ_C 83.0), of H-14 (δ_H 1.48) with C-1 (δ_H 148.2), C-9 (δ_C 36.6), and C-10 (δ_C 77.2), and of H-15 (δ_H 2.19) with C-3 (δ_C 127.7) and C-5 (δ_C 60.2). The position of the methoxy group was assigned by the HMBCs between H-1' (δ_H 3.14) and C-10 (δ_C 77.2). The relative configuration of **12** was determined by its coupling constants and ROESY spectrum (Fig. 3). The large coupling constants of H-5/H-6 ($J_{H\text{-}5/H\text{-}6}$ = 10.6 Hz) and H-6/H-7 ($J_{H\text{-}6/H\text{-}7}$ = 10.5 Hz) indicated their *trans* relationships. The correlations of H-7/H-5 and H-14/H-6 in the ROESY spectrum suggested that H-7 and H-5 were *α*-oriented, whereas H-6 and H-14 were *β*-oriented. The absolute configuration of **12** was established to be 5*S*,6*S*,7*S*,10*R* by comparison of its experimental ECD spectrum with the calculated one (Fig. 4). Therefore, the structure of compound **12** was confirmed as (5*S*,6*S*,7*S*,10*R*)-10-methoxy-guaian-1,3,11(13)-trien-12,6-olide.

Artemdubinoid M (**13**) was assigned a molecular formula of $C_{16}H_{20}O_3$ by the analysis of the (+)-HR-ESI-MS *m/z* 261.1409 $[M + H]^+$ (Calcd. for $C_{16}H_{21}O_3$, 261.1407). Its IR absorption bands at 1767 and 1648 cm^{-1} denoted the existence of carbonyl and olefinic groups. The structure of compound **13** was very similar to that of **12** by comparing their ^{1}H and ^{13}C NMR data (Tables 2 and 3), and the main difference was that compound **13** had one more methylene and olefinic quaternary carbon than **12** and the absence of two methines (one olefinic carbon). This analysis suggested that the Δ^3 double bond in **12** was shifted to Δ^4 in **13**, which was confirmed by the ^{1}H-^{1}H COSY correlations of H-2 (δ_H 6.23)/H-3 (δ_H 2.92) and HMBCs of H-15 (δ_H 1.19) with C-3 (δ_C 45.9), C-4 (δ_C 134.9), and C-5 (δ_C 137.1). The large coupling constant of H-6/H-7 ($J_{H\text{-}6/H\text{-}7}$ = 9.9 Hz) suggested that these protons were *trans*-configured. In the ROESY spectrum, the correlations of H-6/H-1' indicated that the methoxy group was *β*-oriented. The experimental and calculated ECD spectra of **13** were highly similar. Thus, the structure of compound **13** was defined as (6*S*,7*S*,10*S*)-10- methoxy-guaian-1,4,11(13)-trien-12,6-olide.

Artemdubinoid N (**14**) was obtained as a white amorphous powder. Its molecular formula was assigned as $C_{15}H_{20}O_3$ by the analysis of the (+)-HR-ESI-MS *m/z* 249.1494 $[M + H]^+$ (Calcd. for $C_{15}H_{21}O_3$, 249.1485). Detailed analyses of the 1D and 2D NMR spectra of **14** resulted in the establishment of its planar structure, which was identical to that of the reported compound maximilianin [25]. In the ROESY spectrum (Fig. 3), the correlations of H-6/H-14 and H-1/H-6 together with the large coupling constant between H-6 and H-7 ($J_{H\text{-}6/H\text{-}7}$ = 9.9 Hz) proposed that H-1 and H-6 were *β*-oriented. The large coupling constant between H-1 and H-5 ($J_{H\text{-}1/H\text{-}5}$ = 9.6 Hz) suggested that H-5 was *α*-orientated. Its absolute configuration was determined to be 1*S*,5*R*,6*S*,7*S*,10*R* by comparing experimental and calculated ECD spectra. Therefore, the structure of compound **14** was determined to be (1*S*,5*R*,6*S*,7*S*,10*R*)-10-hydroxy-guaian-3,11(13)-dien-12,6-olide.

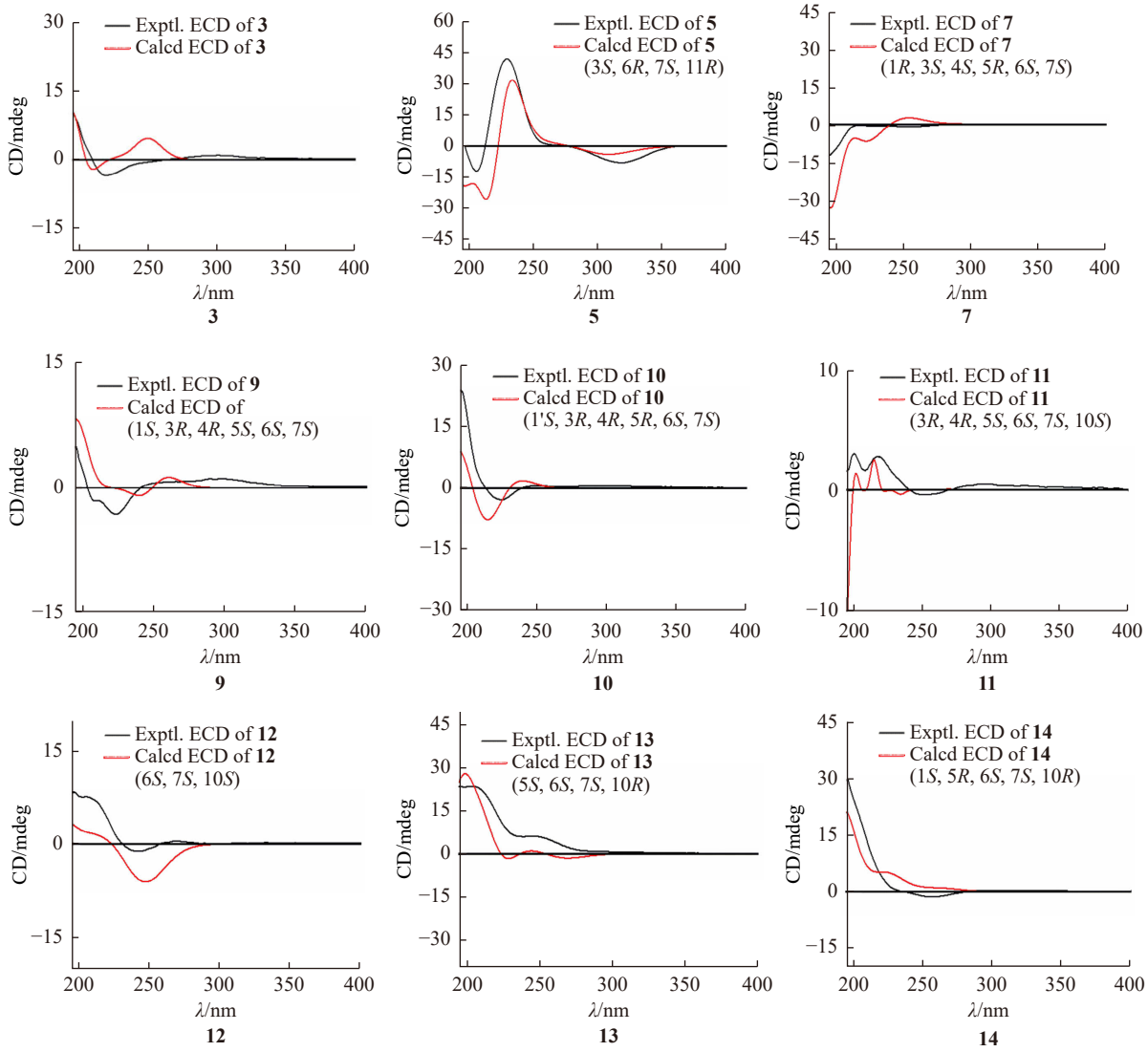

Fig. 4 Experimental and calculated ECD spectra compounds 3, 5, 7, and 9−14.

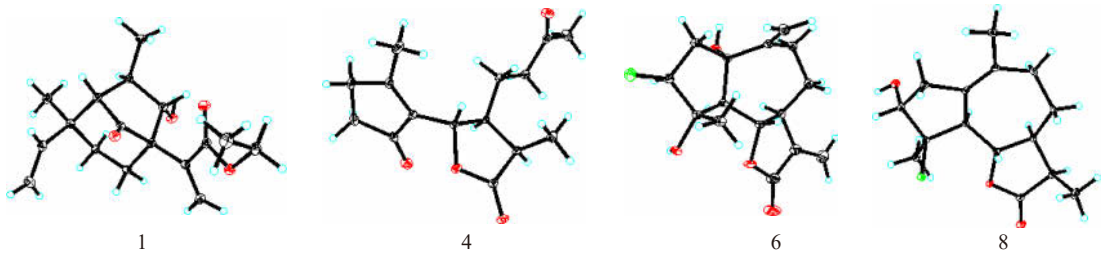

Fig. 5 The X-ray ORTEP drawings of compounds 1, 4, 6 and 8.

Bioassay screening suggested that the EtOAc fraction exhibited cytotoxicity against HepG2 cells with an inhibitory ratio of 84.2% at 100.0 μg·mL^{-1}, which warranted further phytochemical investigation. After separation, the resulting Frs. AD-1–AD-7 from the EtOAc fraction exhibited cytotoxic activity with inhibitory rates of 76.5%, 64.9%, 75.9%, 91.5%, 96.9%, 86.9% and 35.2% at 100.0 μg·mL^{-1}, respectively.

Then 14 previously undescribed sesquiterpenes were isolated from Frs. AD-2 and AD-3 through the activity-guided separation process. All isolated compounds were tested for cytotoxicity at 200 and 100 μmol·L^{-1} against three human hepatoma cell lines (HepG2, Huh7, and SK-Hep-1). Eleven compounds showed inhibitory activity against the three human hepatoma cell lines with inhibitory ratios higher than 80% at 200 μmol·L^{-1}. Detailed cytotoxicity profiling

provided IC_{50} values ranging from 7.5 to 82.5 μmol·L^{-1} (Table 4). Two rare 1,10-*seco*-guaianolides (**4** and **5**) exhibited notable cytotoxicity, with IC_{50} values of 37.1 and 69.9 (HepG2), 66.3 and 64.5 (Huh7), and 44.1 and 72.3 μmol·L^{-1} (SK-Hep-1), respectively. The undescribed guaianolide derivative compound **3** exhibited the cytotoxicity against three human hepatoma cell lines (HepG2, Huh7, and SK-Hep-1) with IC_{50} values of 25.4, 29.8, and 63.6 μmol·L^{-1}, respectively. Compounds **6**, **7**, **9**–**12** and **14** showed moderate cytotoxicity with IC_{50} values ranging from 21.7 to 66.3 μmol·L^{-1}. Among these, compound **13** stood out with IC_{50} values of 14.5, 7.5 and 8.9 μmol·L^{-1} against HepG2, Huh7, and SK-Hep-1 cell lines, which were comparable to those of sorafenib (14.6, 11.3 and 11.2 μmol·L^{-1}). However, the novel structural compounds **1**, **2** and the chlorinated guaiane-type sesquiterpenoid **8** did not exhibit obvious cytotoxic activity against the three human hepatoma cell lines at 100 μmol·L^{-1}.

Experimental

General experimental procedures

See Supporting Information.

Plant material

The plant *Artemisia dubia* Wall. ex Bess was collected from Dali, Yunnan Province, China in September 2019, and was authenticated by Prof. LEI Ligong (Kunming Institute of Botany, Chinese Academy of Sciences, CAS). For reference and future studies, a voucher specimen of the plant was cataloged (No. 20190716-01) in the Laboratory of Antivirus and Natural Medicinal Chemistry, Kunming Institute of Botany, Chinese Academy of Sciences.

Extraction and isolation

The aerial parts of *A. dubia*, after being dried and powdered (20 kg), were soaked in 90% EtOH at room temperature for 12 days, with the solvent being changed every four days. The combined EtOH extracts were then concentrated under reduced pressure, suspended in water, and partitioned with EtOAc, yielding an EtOAc extract weighing 0.75 kg. This extract was subsequently subjected to silica gel column chromatography (Si CC, 8 kg, 200−300 mesh) and eluted with a gradient elution system of acetone and petroleum ether (2 ∶ 98, 5 ∶ 95, 10 ∶ 90, 20 ∶ 80, 30 ∶ 70, 50 ∶ 50, *V*/*V*) to afford seven fractions, AD-1 (181 g), AD-2 (90 g), AD-3 (30 g), AD-4 (50 g), AD-5 (61 g), AD-6 (100 g), and AD-7 (95 g).

Fr. AD-2 (90 g) was further separated on an MCI CHP 20P column and eluted with a H_2O−MeOH gradient (70 ∶ 30, 50 ∶ 50, 30 ∶ 70, 10 ∶ 90), yielding four sub-fractions, AD-2-1−AD-2-4. Fr. AD-2-3 (30 g) was chromatographed on a Si CC by EtOAc−$CHCl_3$ (10 ∶ 90 to 30 ∶ 70) to afford three subfractions: Fr. AD2-3-1−Fr. AD2-3-3. Fr. AD2-3-1 (2.5 g) was subjected to a Sephadex LH-20 CC (140 g, 2.5 cm × 140 cm, MeOH−$CHCl_3$, 50 ∶ 50), followed by semipreparative HPLC (H_2O−MeOH, 25 ∶ 75) to yield compounds **12** (13 mg) and **13** (20 mg). Fr. AD2-3-2 (12 g) was purified by Sephadex LH-20 CC (160 g, 3.0 cm × 150 cm, MeOH−$CHCl_3$, 50 ∶ 50) followed by semipreparative HPLC (H_2O−MeCN, 55 ∶ 45), yielding compounds **3** (50 mg) and **14** (11 mg). The Fr. AD2-3-3 (4.0 g) was submitted to Sepha-

Table 4 Cytotoxicity of compounds 1−14 from *A. dubia* (means ± SD, *n* = 3)

Compounds	IC_{50} (μmol·L^{-1})		
	HepG2	Huh7	SK-Hep-1
1	> 100	> 100	> 100
2	> 100	> 100	> 100
3	25.4 ± 2.9	29.8 ± 1.2	63.6 ± 1.9
4	37.1 ± 1.9	66.3 ± 6.3	44.1 ± 1.4
5	69.9 ± 0.8	64.5 ± 8.8	72.3 ± 3.6
6	67.9 ± 0.8	27.0 ± 1.9	34.7 ± 0.7
7	82.5 ± 2.9	25.7 ± 1.2	36.2 ± 1.9
8	> 100	> 100	> 100
9	21.7 ± 3.9	29.6 ± 4.3	27.7 ± 3.9
10	19.5 ± 2.7	18.2 ± 3.8	14.5 ± 2.7
11	87.8 ± 1.8	> 100	83.8 ± 1.8
12	36.8 ± 0.3	63.9 ± 2.9	36.8 ± 1.2
13	14.5 ± 0.7	7.5 ± 1.0	8.9 ± 1.2
14	21.7 ± 0.2	23.0 ± 0.4	19.2 ± 0.6
Sorafenib[a]	14.6 ± 0.4	11.3 ± 0.5	11.2 ± 0.4

[a]Sorafenib was used as a positive control.

dex LH-20 CC (160 g, 3.0 cm × 150 cm, MeOH−$CHCl_3$, 50 ∶ 50) and purified by semipreparative HPLC (H_2O−MeOH, 30 ∶ 70), yielding compounds **6** (17 mg, t_R = 20.5 min) and **7** (11 mg, t_R = 22.0 min). Similarly, Fr. AD2-3-3 (2.0 g) was purified by Sephadex LH-20 CC and semipreparative HPLC to obtain compounds **10** (6 mg, t_R = 15.0 min) and **11** (15 mg, t_R = 23.5 min).

Fr. AD-3 (30 g) was separated by MPLC on an RP-C18 column with H_2O−MeOH (50 ∶ 50, 30 ∶ 70, 10 ∶ 90) to provide three sub-fractions (AD-3-1−AD-3-3). Fr. AD-3-1 (12 g) was separated on a Si CC (270 g, 6 cm × 25 cm, acetone−petroleum ether, 10 ∶ 90 to 30 ∶ 70) to afford four sub-fractions (AD-3-1-1−AD-3-1-3), of which Fr. AD-3-1-1 (3.5 g) was repeatedly purified by Si CC (40 g, 2.5 cm × 30 cm) using a gradient of EtOAc−$CHCl_3$ (10 ∶ 90 to 20 ∶ 80) to afford compounds **8** (14 mg) and **9** (3 mg). Fr. AD-3-1-2 (3.0 g) was subjected to Si CC (45 g, 4.0 cm × 25 cm, EtOAc−$CHCl_3$, 10 ∶ 90), followed by Sephadex LH-20 CC (160 g, 2.5 cm × 175 cm, MeOH−$CHCl_3$, 50 ∶ 50) and semi-preparative HPLC (H_2O−MeCN, 35 ∶ 65, 10.0 mL·min^{-1}), yielding compounds **1** (30 mg, t_R = 12.5 min) and **2** (12 mg, t_R = 18.5 min). Fr. AD-3-1-3 (3.0 g) was subjected to Si CC (60 g, 4.0 cm × 25 cm, EtOAc−$CHCl_3$, 10 ∶ 90) followed by semipreparative HPLC (H_2O−MeOH, 30 ∶ 70, 3.0 mL·min^{-1}) to obtain compounds **4** (25 mg, t_R = 15.5 min) and **5** (13 mg, t_R = 23.5 min).

Artemdubinoid A (**1**): orthorhombic crystals (MeOH–$CHCl_3$, 5 ∶ 95); mp 131−132 ºC; $[\alpha]_D^{22}$ +15.4 (*c* 0.06, MeOH); ECD (MeOH) λ_{max} ($\Delta\varepsilon$) 205 (+0.19), 226 (+2.00) nm; IR ν_{max} 3436, 1743, 1715, 1625, 1373, 1283, 1179, 1048 cm^{-1}; ^1H and ^{13}C NMR data (Tables 1 and 3); (+)-HR-ESI-MS *m/z* 293.174 4 $[M + H]^+$ (Calcd. for $C_{17}H_{25}O_4$, 293.174 7).

Artemdubinoid B (**2**): whiter powder; $[\alpha]_D^{22}$ +32.1 (*c* 0.07, MeOH); ECD (MeOH) λ_{max} ($\Delta\varepsilon$) 205 (–3.96), 229 (+11.65) nm; IR ν_{max} 3458, 1739, 1722, 1628, 1371, 1283, 1165, 1049 cm^{-1}; ^1H and ^{13}C NMR data (Tables 1 and 3); (+)-HR-ESI-MS *m/z* 279.159 6 $[M + H]^+$ (Calcd. for $C_{16}H_{23}O_4$, 279.159 1).

Artemdubinoid C (**3**): colorless oil; $[\alpha]_D^{22}$ +17.5 (*c* 0.03, MeOH); ECD (MeOH) λ_{max} ($\Delta\varepsilon$) 216 (+1.89) nm; IR ν_{max} 3439, 1758, 1706, 1266, 1219, 1099 cm^{-1}; ^1H and ^{13}C NMR data (Tables 1 and 3); (–)-HR-ESI-MS *m/z* 417.228 7 $[M + HCOO]^-$ (Calcd. for $C_{24}H_{33}O_6$, 417.228 3).

Artemdubinoid D (**4**): monoclinic crystals (MeOH–$CHCl_3$, 5 ∶ 95); mp 112−113 ºC; $[\alpha]_D^{22}$ +40.6 (*c* 0.05, MeOH); ECD (MeOH) λ_{max} ($\Delta\varepsilon$) 243 (+ 0.36) nm; IR ν_{max} 1771, 1699, 1648, 1383, 1260, 1211, 1079 cm^{-1}; ^1H and ^{13}C NMR data see Tables 1 and 3; (+)-HR-ESI-MS *m/z* 287.123 0 $[M + Na]^+$ (Calcd. for $C_{15}H_{20}O_4Na$, 287.125 4).

Artemdubinoid E (**5**): whiter powder; $[\alpha]_D^{22}$ +38.8 (*c* 0.10, MeOH); ECD (MeOH) λ_{max} ($\Delta\varepsilon$) 210 (+5.99), 252 (–0.84) nm; IR ν_{max} 3433, 1770, 1707, 1651, 1383, 1262, 1210, 1052 cm^{-1}; ^1H and ^{13}C NMR data (Tables 1 and 3); (–)-HR-ESI-MS *m/z* 325.128 4 $[M + HCOO]^-$ (Calcd. for $C_{16}H_{21}O_7$, 325.129 3).

Artemdubinoid F (**6**): orthorhombic crystals (MeOH–$CHCl_3$, 5 ∶ 95); mp 118−119 ºC; $[\alpha]_D^{22}$ +92.8 (*c* 0.10, MeOH); ECD (MeOH) λ_{max} ($\Delta\varepsilon$) 195 (–369) nm; IR ν_{max} 3346, 1763, 1634, 1381, 1288, 1196, 1072cm^{-1}; ^1H and ^{13}C NMR data (Tables 1 and 3); (+)-HR-ESI-MS *m/z* 321.085 2 $[M + Na]^+$ (Calcd. for $C_{15}H_{19}O_4Cl$ Na, 321.086 4).

Artemdubinoid G (**7**): whiter powder; $[\alpha]_D^{22}$ –10.0 (*c* 0.08, MeOH); ECD (MeOH) λ_{max} ($\Delta\varepsilon$) 195 (+12.89) nm; IR ν_{max} 3426, 1758, 1634, 1384, 1263, 1202, 1072 cm^{-1}; ^1H and ^{13}C NMR data (Tables 1 and 3); (+)-HR-ESI-MS *m/z* 321.0853 $[M + Na]^+$ (Calcd. for $C_{15}H_{19}O_4Cl$ Na, 321.086 4).

Artemdubinoid H (**8**): orthorhombic crystals (MeOH–$CHCl_3$, 5 ∶ 95); mp 117−118 ºC; $[\alpha]_D^{22}$ +74.5 (*c* 0.09, MeOH); ECD (MeOH) λ_{max} ($\Delta\varepsilon$) 208 (–10.8) nm; IR ν_{max} 3495, 1753, 1378, 1261, 1219, 1042 cm^{-1}; ^1H and ^{13}C NMR data (Tables 2 and 3); (+)-HR-ESI-MS *m/z* 285.127 2 $[M + H]^+$ (Calcd. for $C_{15}H_{22}O_3Cl$, 285.125 2).

Artemdubinoid I (**9**): whiter powder; $[\alpha]_D^{22}$ –33.8 (*c* 0.09, MeOH); ECD (MeOH) λ_{max} ($\Delta\varepsilon$) 224 (+0.74) nm; IR ν_{max} 3435, 1764, 1640, 1384, 1261, 1227, 1057 cm^{-1}; ^1H and ^{13}C NMR data (Tables 2 and 3); (+)-HR-ESI-MS *m/z* 283.112 1 $[M + H]^+$ (Calcd. for $C_{15}H_{20}O_3Cl$, 283.109 5).

Artemdubinoid J (**10**): whiter powder; $[\alpha]_D^{22}$ +33.0 (*c* 0.10, MeOH); ECD (MeOH) λ_{max} ($\Delta\varepsilon$) 224 (+ 0.79) nm; IR ν_{max} 3432, 1759, 1635, 1379, 1259, 1218, 1082 cm^{-1}; ^1H and ^{13}C NMR data (Tables 2 and 3); (+)-HR-ESI-MS *m/z* 299.105 7 $[M + H]^+$ (Calcd. for $C_{15}H_{20}O_4Cl$, 299.104 5).

Artemdubinoid K (**11**): whiter powder; $[\alpha]_D^{22}$ –52.2 (*c* 0.09, MeOH); ECD (MeOH) λ_{max} ($\Delta\varepsilon$) 224 (+0.74) nm; IR ν_{max} 3424, 1759, 1633, 1382, 1261, 1203, 1082 cm^{-1}; ^1H and ^{13}C NMR data (Tables 2 and 3); (+)-HR-ESI-MS *m/z* 299.106 0 $[M + H]^+$ (Calcd. for $C_{15}H_{20}O_4Cl$, 299.104 5).

Artemdubinoid L (**12**): whiter powder; $[\alpha]_D^{22}$ –17.7 (*c* 0.15, MeOH); ECD (MeOH) λ_{max} ($\Delta\varepsilon$) 234 (–2.25) nm; IR ν_{max} 1767, 1437, 1255, 1224, 1093 cm^{-1}; ^1H and ^{13}C NMR data (Tables 2 and 3); (+)-HR-ESI-MS *m/z* 261.111 0 $[M + H]^+$ (Calcd. for $C_{16}H_{21}O_3$, 261.112 1).

Artemdubinoid M (**13**): whiter powder; $[\alpha]_D^{22}$ +39.1 (*c* 0.11, MeOH); ECD (MeOH) λ_{max} ($\Delta\varepsilon$) 229 (+13.15) nm; IR ν_{max} 1765, 1666, 1448, 1298, 1281, 1013 cm^{-1}; ^1H and ^{13}C NMR data (Tables 2 and 3); (+)-HR-ESI-MS *m/z* 261.140 9 $[M + H]^+$ (Calcd. for $C_{16}H_{21}O_3$, 261.140 7).

Artemdubinoid N (**14**): whiter powder; $[\alpha]_D^{22}$ +38.6 (*c* 0.10, MeOH); ECD (MeOH) λ_{max} ($\Delta\varepsilon$) 195 (+8.86) nm; IR ν_{max} 3436, 1758, 1664, 1376, 1264, 1228, 1110 cm^{-1}; ^1H and ^{13}C NMR data (Tables 2 and 3); (+)-HR-ESI-MS *m/z* 249.149 4 $[M + H]^+$ (Calcd. for $C_{15}H_{21}O_3$, 249.148 5).

*X-ray crystallographic analysis of compounds **1**, **4**, **6** and **8***

Compounds **1**, **6** and **8**, orthorhombic crystals, were afforded by recrystallization in a mixture of MeOH–$CHCl_3$ (5 ∶ 95). Compound **4**, a monoclinic crystal, was obtained by recrystallization in a mixture of MeOH–$CHCl_3$ (5 ∶ 95). X-ray diffraction analyses were conducted on a Bruker D8 QUEST instrument using Cu Kα radiation, and the intensity

data were collected at 100(2) K. The initial solution of the crystal structures was carried out with SHELXS-97 and difference Fourier techniques. Further refinements were made through full-matrix least-squares calculations on F2, an approach that allows for the precise determination of atom positions and thermal vibrations. All nonhydrogen atoms were anisotropically refined, and the positions of hydrogens bonded to carbons were initially determined through geometry and refined using a riding model. The crystallographic data for compounds **1**, **4**, **6** and **8** in standard CIF format were deposited in the Cambridge Crystallographic Data Centre and made publicly available at http://www.ccdc.cam.ac.uk/.

Crystal data for compound ***1***: $C_{17}H_{24}O_4$, M = 292.36, a = 6.6265(2) Å, b = 7.7284(2) Å, c = 30.0059(7) Å, α = 90°, β = 90°, γ = 90°, V = 1536.67(7) Å^3, T = 100.(2) K, space group P212121, Z = 4, μ(Cu Kα) = 0.718 mm^{-1}, 15112 measured reflections, 3037 independent reflections (R_{int} = 0.0342). The final R_1 values were 0.0265 ($I > 2\sigma(I)$). The final $wR(F^2)$ values were 0.0681 ($I > 2\sigma(I)$). The final R_1 values were 0.0265 (all data). The final $wR(F^2)$ values were 0.0681 (all data). The goodness of fit on F^2 was 1.065. Flack parameter = 0.01(3). CCDC 2142229.

Crystal data for compound ***4***: $C_{15}H_{20}O_4$, M = 264.31, a = 9.8718(4) Å, b = 6.9522(3) Å, c = 11.1732(4) Å, α = 90°, β = 112.2970(10)°, γ = 90°, V = 709.49(5) Å^3, T = 100.(2) K, space group P1211, Z = 2, μ(Cu Kα) = 0.727 mm^{-1}, 14833 measured reflections, 2733 independent reflections (R_{int} = 0.0319). The final R_1 values were 0.0258 ($I > 2\sigma(I)$). The final $wR(F^2)$ values were 0.0675 ($I > 2\sigma(I)$). The final R_1 values were 0.0259 (all data). The final $wR(F^2)$ values were 0.0676 (all data). The goodness of fit on F^2 was 1.075. Flack parameter = 0.06(4). CCDC 2142238.

Crystal data for compound ***6***: $C_{15}H_{19}O_4Cl$, M = 298.75, a = 7.1058(2) Å, b = 12.4178(3) Å, c = 16.7218(4) Å, α = 90°, β = 90°, γ = 90°, V = 1475.50(7) Å^3, T = 101.(2) K, space group P212121, Z = 4, μ(Cu Kα) = 2.390 mm^{-1}, 13784 measured reflections, 2886 independent reflections (R_{int} = 0.0358). The final R_1 values were 0.0265 ($I > 2\sigma(I)$). The final $wR(F^2)$ values were 0.0681 ($I > 2\sigma(I)$). The final R_1 values were 0.0269 (all data). The final $wR(F^2)$ values were 0.0684 (all data). The goodness of fit on F^2 was 1.057. Flack parameter = 0.054(6). CCDC 2142233.

Crystal data for compound ***8***: $C_{15}H_{21}O_3Cl$, M = 284.77, a = 8.8574(2) Å, b = 10.5511(3) Å, c = 15.1808(4) Å, α = 90°, β = 90°, γ = 90°, V = 1418.73(6) Å^3, T = 100.(2) K, space group P212121, Z = 4, μ(Cu Kα) = 2.401 mm^{-1}, 11866 measured reflections, 2761 independent reflections (R_{int} = 0.0475). The final R_1 values were 0.0320 ($I > 2\sigma(I)$). The final $wR(F^2)$ values were 0.0803 ($I > 2\sigma(I)$). The final R_1 values were 0.0323 (all data). The final $wR(F^2)$ values were 0.0805 (all data). The goodness of fit on F^2 was 1.096. Flack parameter = 0.089(7). CCDC 2142712.

Cytotoxicity assay

The antihepatoma activity of the compounds extracted from *A. dubia* was measured by a 3-(4,5-dimethylthiazol-2-yl)-2,5-diphenyltetrazolium bromide (MTT) assay on three human hepatocellular carcinoma cell lines (HepG2, Huh7, and SK-Hep-1). The cells were initially seeded in a 96-well plate at a density of 1 × 10^4 cells per well and incubated in a controlled environment with 5% CO_2 at 37 °C for 24 h. Following this incubation period, the samples of the isolated compounds at different concentrations were added to the cells. The cells were then further incubated for 48 h under the same conditions. Afterwards, 100 μL of the MTT solution (1 mg·mL^{-1}) was added to each well. The cells were incubated with MTT for 4 h at 37 °C. Then the liquid containing unconverted MTT was then discarded, and 100 μL of DMSO was added to dissolve the MTT formazan salt. The absorbance was measured using a microplate reader (BIO-RAD, USA) at 490 nm. The inhibitory rates were calculated as $[A_{(control)} - A_{(sample)}]/A_{(control)} \times 100\%$, and IC_{50} values were calculated by GraphPad Prism 7 (GraphPad Software, San Diego, CA, USA). All results and data were expressed as the mean ± SD of three independent experiments.

ECD calculations for compounds ***3***, ***5***, ***7***, *and* ***12–14***

The ECD spectra of compounds **3**, **5**, **7**, and **12**–**14** were calculated with Gaussian 09 software. The relative configurations of compounds **3**, **5**, **7**, and **12**–**14** were determined from their ROESY experiments and optimized in the gas phase by DFT calculation at the B3lyp/6-31G(d,p) level. To ensure that the ECD spectral calculations were based on realistic molecular vibrations, we performed frequency calculations at the same level of theory. Further refinement in the ECD spectral prediction came from time-dependent DFT (TDDFT) calculations at the b3lyp/6-311 + g(d,p) level with the consideration of solvent effects. Finally, the resultant ECD spectral data were graphically represented using Origin Pro 9 software (OriginLab Corporation, Northampton, MA, USA).

Conclusion

In summary, the investigation led to the discovery of fourteen undescribed sesquiterpenoids from *A. dubia*, including two novel sesquiterpenoids featuring a 6/5-fused bicyclic scaffold (**1**–**2**) and 12 new guaiane-type ones (**3**–**14**). The structural elucidation of these compounds was achieved through comprehensive spectral data analysis and ECD calculation methods and confirmed with single-crystal X-ray diffraction. The bioactivity assessment revealed that 11 of the compounds showed inhibitory activity against HepG2, Huh7, and SK-Hep-1 cell lines with IC_{50} values ranging from 7.5 to 82.5 μmol·L^{-1}, with compound **13** demonstrating particularly strong inhibitiona against the three cell lines, with IC_{50} values of 14.5, 7.5 and 8.9 μmol·L^{-1}, respectively. By isolating and characterizing new bioactive sesquiterpenoids, this study adds depth to the understanding of *A. dubia* and supports the ongoing search for novel antihepatoma agents within the *Artemisia* genus.

Supplementary material

Supplementary data for this article can be abtained by

sending an E-mail to corresponding author.

References

[1] Tang S, Zhang XT, Ma YB, *et al*. Artemyrianolides A–S, cytotoxic sesquiterpenoids from *Artemisia myriantha* [J]. *J Nat Prod*, 2020, **83**(9): 2618-2630.

[2] Lee SE, Sivtseva S, Lim C, *et al*. Artemisia kruhsiana leaf extract induces autophagic cell death in human prostate cancer cells [J]. *Chin J Nat Med*, 2021, **19**(2): 134-142.

[3] Wang Q, Zhang T, Ke CQ, *et al*. Guaianolides from *Artemisia codonocephala* suppress interleukine-1*β* secretion in macrophages [J]. *Phytochemistry*, 2021, **192**: 112955.

[4] Qin DP, Li T, Shao JR, *et al*. Arteannoides U–Z: six undescribed sesquiterpenoids with anti-inflammatory activities from the aerial parts of *Artemisia annua* (Qinghao) [J]. *Fitoterapia*, 2021, **154**: 105002.

[5] Wang X, Peng X, Tang C, *et al*. Anti-inflammatory eudesmane sesquiterpenoids from *Artemisia hedinii* [J]. *J Nat Prod*, 2021, **84**(5): 1626-1637.

[6] Sun YW, Ju Y, Liu CH, *et al*. Polyhydroxyl guaianolide terpenoids as potential NF-*κ*B inhibitors induced cytotoxicity in human gastric adenocarcinoma cell line [J]. *Bioorg Chem*, 2020, **95**: 103551.

[7] Shi XS, Li HL, Li XM, *et al*. Highly oxygenated polyketides produced by Trichoderma koningiopsis QA-3, an endophytic fungus obtained from the fresh roots of the medicinal plant *Artemisia argyi* [J]. *Bioorg Chem*, 2020, **94**: 103448.

[8] Jiang Z, Guo X, Zhang K, *et al*. The essential oils and eucalyptol from *Artemisia vulgaris* L. prevent acetaminophen-induced liver injury by activating Nrf2–Keap1 and enhancing APAP clearance through non-toxic metabolic pathway [J]. *Front Pharmacol*, 2019, **10**: 782.

[9] Argemi X, Hansmann Y, Gaudart J, *et al*. Comment on "effect of *Artemisia annua* and *Artemisia afra* tea infusions on schistosomiasis in a large clinical trial" [J]. *Phytomedicine*, 2019, **62**: 152804.

[10] Daddy NB, Kalisya LM, Bagire PG, *et al*. *Artemisia annua* dried leaf tablets treated malaria resistant to ACT and i. v. artesunate: case reports [J]. *Phytomedicine*, 2017, **32**: 37-40.

[11] Efferth T, Herrmann F, Tahrani A, *et al*. Cytotoxic activity of secondary metabolites derived from *Artemisia annua* L. towards cancer cells in comparison to its designated active constituent artemisinin [J]. *Phytomedicine*, 2011, **18**(11): 959-969.

[12] Zhu C, Shi H, Wu M, *et al*. A dual MET/AXL small-molecule inhibitor exerts efficacy against gastric carcinoma through killing cancer cells as well as modulating tumor microenvironment [J]. *Med Comm*, 2020, **1**(1): 103-118.

[13] Krishna S, Bustamante L, Haynes RK, *et al*. Artemisinins: their growing importance in medicine [J]. *Trends Pharmacol Sci*, 2008, **29**(10): 520-527.

[14] Ivanescu B, Miron A, Corciova A. Sesquiterpene lactones from *Artemisia* genus: biological activities and methods of analysis. [J]. *J Anal Methods Chem*, 2015, **2015**: 247685.

[15] Tang JJ, He QR, Dong S, *et al*. Diversity modification and structure-activity relationships of two natural products 1*β*-hydroxy alantolactone and ivangustin as potent cytotoxic agents [J]. *Sci Rep*, 2018, **8**(1): 1722.

[16] Su L, Zhang X, Ma Y, *et al*. New guaiane-type sesquiterpenoid dimers from *Artemisia atrovirens* and their antihepatoma activity [J]. *Acta Pharm Sin B*, 2020, **11**(6): 1648-1666.

[17] Zhang XT, Hu J, Su LH, *et al*. Artematrolide A inhibited cervical cancer cell proliferation *via* ROS/ERK/mTOR pathway and metabolic shift [J]. *Phytomedicine*, 2021, **91**: 153707.

[18] Su LH, Geng CA, Li TZ, *et al*. Artatrovirenols A and B: Two cagelike sesquiterpenoids from *Artemisia atrovirens* [J]. *J Org Chem*, 2020, **85**(21): 13466-13471.

[19] Su LH, Ma YB, Geng CA, *et al*. Artematrovirenins A–P, guaiane-type sesquiterpenoids with cytotoxicities against two hepatoma cell lines from *Artemisia atrovirens* [J]. *Bioorg Chem*, 2021, **114**: 105072.

[20] Tang S, Ma YB, Geng CA, *et al*. Artemyrianins A–G from *Artemisia myriantha* and their cytotoxicity against HepG2 cells [J]. *Nat Prod Bioprospect*, 2020, **10**(4): 10.

[21] Huang ZS, Pei YH, Liu CM, *et al*. Highly oxygenated guaianolides from *Artemisia dubia* [J]. *Planta Med*, 2010, **76**(15): 1710-1716.

[22] Ahmed AA, Gáti T, Hussein TA, *et al*. Ligustolide A and B, two novel sesquiterpenes with rare skeletons and three 1,10-*seco*-guaianolide derivatives from *Achillea ligustica*. [J]. *Tetrahedron*, 2003, **59**: 3729-3735.

[23] Ahmed, El-Moghazy SA, El-Shanawany MA, *et al*. Polyol monoterpenes and sesquiterpene lactones from the Pacific Northwest plant *Artemisia suksdorfii* [J]. *J Nat Prod*, 2004, **67**(10): 1705-1710.

[24] Zhao P, Xin BS, Qin SY, *et al*. Characteristic guaiane sesquiterpenes from *Daphne penicillata* and ECD/NMR-based assignment of C-1 configuration [J]. *Org Chem Front*, 2022, **9**(22): 6213-6222.

[25] Miyase T, Kuroyanagi M, Noro T, *et al*. Studies on sesquiterpenes from *Macroclinidium trilobum* MAKINO. II [J]. *Chem Pharm Bull*, 1985, **33**(10): 4445-4450.

Cite this article as: GAO Zhen, LI Tianze, MA Yunbao, HUANG Xiaoyan, GENG Changan, ZHANG Xuemei, CHEN Jijun. Artemdubinoids A–N: novel sesquiterpenoids with antihepatoma cytotoxicity from *Artemisia dubia* [J]. *Chin J Nat Med*, 2023, **21**(12): 902-915.